

Non-Linear Thermal Model for Transformers Study

MARIUS CONSTANTIN POPESCU¹NIKOS E. MASTORAKIS²CORNELIA AIDA BULUCEA¹GHEORGHE MANOLEA¹LILIANA PERESCU-POPESCU³

¹ Faculty of Electromechanical and Environmental Engineering, University of Craiova
ROMANIA

² Military Institutes of University Education, Hellenic Naval Academy
GREECE

³ Charles Logier College Craiova
ROMANIA

popescu.marius.c@gmail.com, mastorakis4567@gmail.com, abulucea@gmail.com, ghmanolea@gmail.com,

Abstract: This article begins with a study of transformer additional losses due to the presence of non-sinusoidal loads, presents existing models to represent these losses and proposes an original model. Consequent increment in transformer loss of life is studied by means of a sensitivity analysis of the model to transformer rated power, load amplitude, thermal inertia, profiles correlation and harmonic spectrum content.

Key-Words: Transformer model, Non-sinusoidal loads, Thermal parameters

1 Introduction

The proliferation of non-linear loads causes a harmonic distortion on public and industrial networks. The transformers thermal ageing, estimated for sinusoidal loads, may increase if harmonic currents are considered. This is the main subject of this chapter. Transformer additional losses due to power supply distortion can reside both on voltage and current harmonics. On section §2, the variation of additional losses with frequency is analysed. Additional losses of a set of conductors located on an equivalent slot are determined and comparisons for several equivalent cross sections of conductors are presented. The influence between currents of adjacent conductors plays a determinant role on additional losses determination since they limit, in frequency, the reduction in losses achieved by sub-dividing large cross section conductors. These results are also illustrated with graphs of conductor's current density for different frequencies. Models obtained for losses generated on conductors placed on slots are generalised for transformer windings with rectangular cross section conductors. The models of these additional losses, presented on section §2, are difficult to parameterise since they require a detailed knowledge of transformer electric and magnetic circuits. In the specialised literature several simplified versions which validity is, limited in frequency, can be found. A new model of transformer additional losses due to current harmonics is presented. The proposed model is not

frequency limited and is easy to parameterise since it relies only on the transformer rated power. The proposed model is compared with existing ones to evidence the achieved improvements.

2 Transformer Losses Driving Non-Sinusoidal Loads

Transformer total losses can be separated into no-load losses, also referred as core losses related to the voltage, and load losses, also referred as winding losses related to the current. No-load losses comprise hysteresis and eddy current losses in the transformer magnetic core. These losses are related to permeability and conductivity of core magnetic material, the core lamination and design and also to the magnetic induction field, which in turn depends upon the applied voltage [1],[2]. As a consequence of voltage distortion on the transformer power supply, no load losses will be affected, relatively to losses generated under a purely sinusoidal voltage. International Standards [3],[4], impose that for distribution transformers, harmonic distortion on the power system voltage must be below 5%, apart excessive harmonic loading or resonance conditions [5],[6]. Under these conditions and having the MV power system a higher internal short-circuit power than the rated apparent power of the considered transformer, the frequency of the applied voltage is predominantly the fundamental. Thus, the voltage distortion level will not induce significant additional no-load losses and no correction is needed on no-load losses due

to voltage harmonics [4]. According to [7] a 10% distortion on the applied voltage will lead to an increase on no-load losses of about 1% only, relatively to rated values. Under these conditions, the main influence of harmonics on transformer losses will be reflected on load losses. The most significant load losses arise from the flowing of load current through the windings resistance but, since time varying fields are involved, additional losses (stray losses) arise from eddy-currents due to stray electromagnetic flux in transformer electric conducting materials (windings, core, core clamps, magnetic shields, tank walls). Although all these losses contribute to increase transformer temperature, stray losses occurring in windings of distribution transformers are considered critical, [8],[9]. Windings stray losses, although not so significant at rated sinusoidal load (around 10% of total load losses [9]), can be determinant under a non-sinusoidal environment, due to its significant increase with frequency.

3 Stray Loss Variations with frequency

3.1 Losses Formulation

Under rated conditions (this rated regime being denoted by the sub-script 1) transformer load losses on windings can be traduced by:

$$P_{WIN1} = R_{AC1} I_1^2, \quad (1)$$

where: R_{AC1} transformer apparent resistance associated to DC current and AC current at fundamental frequency [Ω]; I_1 rated load current (RMS) at rated frequency [A].

Introducing an apparent resistance associated to eddy losses at fundamental frequency, ΔR_1 , expression (1) can also be written as

$$P_{WIN1} = R_{DC} \beta_1 I_1^2, \quad (2)$$

being, by definition:

$$\beta_1 = \left(1 + \frac{\Delta R_1}{R_{DC}} \right), \quad (3)$$

where: R_{DC} transformer equivalent resistance associated to DC current and taking into account the real winding temperature [Ω].

Under a non-sinusoidal load current environment, the total current flowing on the windings is:

$$I = \sqrt{\sum_{h=1} I_h^2}, \quad (4)$$

with: I , load current (RMS) [A], I_h , load current (RMS) at harmonic order h [A] and thus, generalisation of (1) for a non-sinusoidal load current, will lead to:

$$P_{WINh} = \sum_{h=1} R_{ACh} I_h^2 = R_{DC} \sum_{h=1} \beta_h I_h^2, \quad (5)$$

where the transformer apparent resistance R_{ACh} is given by:

$$R_{ACh} = R_{DC} \left(1 + \frac{\Delta R_h}{R_{DC}} \right) \quad (6)$$

and ΔR_h represent an apparent resistance associated to eddy losses at harmonic order h .

As transformers are projected to drive sinusoidal currents at rated frequency (rated regime), it would be useful that additional losses due to the non-sinusoidal current were expressed as a function of losses generated under the rated regime. From (5) it can be derived:

$$P_{WINh} = \beta_1 R_{DC} I_1^2 \left(1 + \frac{\sum_{h=2} \beta_h I_h^2}{\beta_1 I_1^2} \right), \quad (7)$$

where the second term in the parenthesis represents additional losses, due to the non-sinusoidal current, in. p.u. values of losses generated under the rated regime.

Correct analytical determination of (7) is complex. Since time varying fields are involved, additional losses arise from non-uniform distribution of current inside conductors (skin effect) and therefore, the concept of spatially distributed currents must be introduced. Detailed knowledge of transformer electrical and magnetic circuits is required which depends upon many transformer specific characteristics such as: rated power, electric and magnetic material characteristics, windings and conductors geometry and manufacturing structure.

3.2 Skin Effect in Slot Placed Conductors

To take into account the skin effect, the simplification of considering windings as line reduced conductors must be withdraw, since skin effect represents a non-uniform distribution of current density inside conductors. Maxwell's equations must be considered, to analyse spatial current distributions. Figure 1 represents the cross section of a set with m conductors, each one electrically insulated from the others and placed in a slot of a ferromagnetic material. The permeability, to simplify the discussion, is assumed to be infinite compared with that of the air. Slot width is denoted by w_s , conductor width by w_c and conductor height by e . If the conductors length is assumed to be long enough compared to cross section dimensions, so that end effects can be neglected, the three-dimensional circuit can be reduced to a two dimensional circuit (x and z

according to Figure 1).

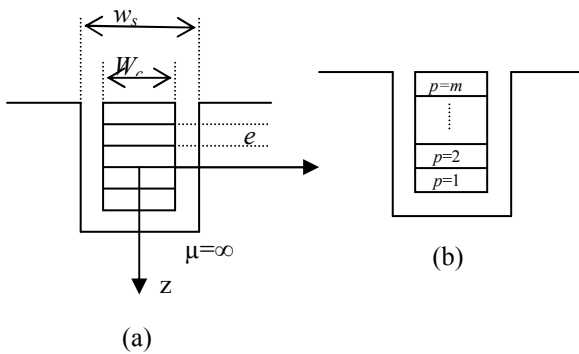


Fig. 1: a) conductors placed in a slot and b) nomenclature of conductor's position in the slot.

Time variations of electric and magnetic fields are assumed to be sinusoidal with angular frequency

$$\omega = h\omega_1 \quad (8)$$

where: ω rated angular frequency [rad.s⁻¹] and h harmonic order.

Considering that every conductor is carrying the same total current, it can be shown [9] that the resistance of each conductor, denoted by R_p , will depend upon its position p in the slot, Figure 1 (b), according to:

$$\frac{R_p}{R_{DCp}} = \xi \frac{\sinh(2\xi) + \sin(2\xi)}{\cosh(2\xi) - \cos(2\xi)} + p(p-1)2\xi \frac{\sinh(\xi) - \sin(\xi)}{\cosh(\xi) + \cos(\xi)} \quad (9)$$

where: R_{DCp} represent the DC resistance of each conductor; for a conductor of length l_c , its DC resistance is given by:

$$R_{DCp} = \frac{l_c}{\gamma_w w_c e} \quad (10)$$

The variable ξ , represents the reduced conductor width [8],[9] and is given by:

$$\xi = \frac{e}{\delta} \sqrt{\frac{w_c}{w_s}}, \quad (11)$$

being δ the penetration depth given by:

$$\delta = \sqrt{\frac{2}{\gamma_w \mu_0 \omega_1}} \sqrt{\frac{1}{h}} \quad (12)$$

The permeability of conductor's material is assumed to be the permeability of vacuum, denoted by μ_0 . The penetration depth is a measure of how deeply each current harmonic is distributed in the conductor and, therefore, the spatial distribution of the magnetic field. If δ is much greater than conductor width e , the current and magnetic field tend to a spatial uniform distribution (DC limit case). At high frequencies δ decreases, Figure 2 (a), and the majority of the current is carried near the surfaces of each conductor, Figure 2 (b), which can be traduced by a reduction in the conductor cross section that effectively carries the current.

This effect is referred on literature as skin effect. To the skin effect contributes not only the conductor current itself, but also the currents of adjacent conductors. This is traduced by the second term of (9). The contribution of adjacent currents to skin effect occurring in a conductor is often referred as proximity effect. To reduce skin effect, large cross section conductors are sectionalised into parallel conductors conveniently twisted and/or transposed so that each sub-conductor will experience equally the eddy effect due to different p positions. If twisting or transposing was not carried out, asymmetries between sub-conductors would arise and the paralleling of them at the end of the layer would allow the circulation of eddy currents and, therefore, annul the expected improvement by subdividing the large cross section conductor. For the conductors represented on Figure 1 being correctly transposed, each portion l_c / m of the conductors total length, l_c , must occupy all possible p positions and, therefore, its resistance will not depend upon its position in the slot but only upon the number of total conductors/transpositions, m .

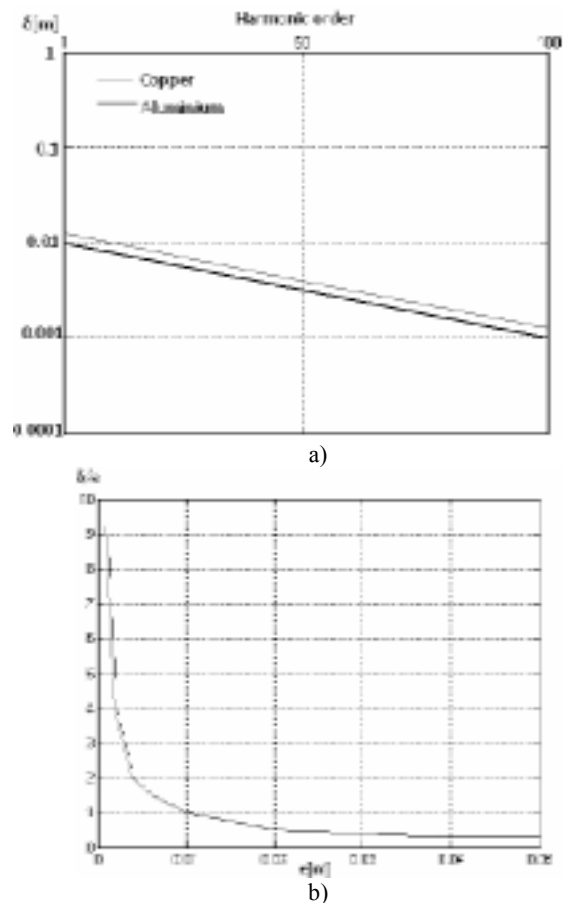


Fig. 2: a) Penetration depth as a function of harmonic order, on 50 Hz per unit base, for copper and aluminium; b) Penetration depth of 50 Hz referred to conductor's height. Copper conductor.

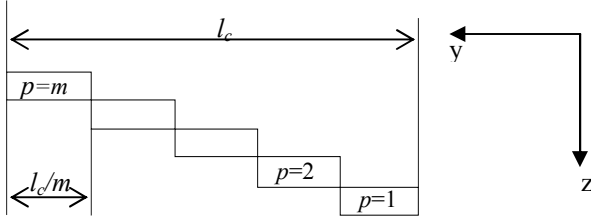


Fig. 3: Diagram representing the longitudinal section of one conductor with m transpositions.

Under these conditions, one can consider that each conductor total resistance, R_{pT} , will be given by the serial resistance of width portions l_c/m of the conductor, denoted by $R_{portion}$, each one placed at different p positions in the slot, Figure 3. It will be:

$$\frac{R_{portion}}{R_{DCportion}} = \varphi(\xi) + p(p-1)\psi(\xi), \quad (13)$$

where: $\varphi(\xi) = \xi \frac{\sinh(2\xi) + \sin(2\xi)}{\cosh(2\xi) - \cos(2\xi)}$ and

$$\psi(\xi) = \xi \frac{\sinh(2\xi) - \sin(2\xi)}{\cosh(2\xi) + \cos(2\xi)} \quad (14)$$

and the DC resistance is given by:

$$R_{DCportion} = \frac{l_c/m}{\gamma_w w_c e}. \quad (15)$$

The serial resistance of the m portions will be given by:

$$R_{pT} = \sum_{p=1}^m R_{portion} = R_{DCportion} m \left(\varphi(\xi) + \frac{m^2-1}{3} \psi(\xi) \right). \quad (16)$$

Since, from (10) and (15), it is:

$$R_{DCportion} m = R_{DCp}, \quad (17)$$

expression (16) is equivalent to:

$$R_{pT} = R_{DCp} \left(\varphi(\xi) + \frac{m^2-1}{3} \psi(\xi) \right). \quad (18)$$

The conductor total resistance, R_{pT} , can also be obtained by considering it as an average of the resistances a conductor length l_c presents at each position p , R_p , given by (9).

$$R_{pT} = \frac{1}{m} \sum_{p=1}^m R_p = R_{DCp} \left(\varphi(\xi) + \frac{m^2-1}{3} \psi(\xi) \right). \quad (19)$$

To realise the improvements and the limits achieved in stray loss reduction by subdividing conductors with large cross section, a numerical example is presented.

3.2.1 Numerical Example

Losses generated on a single conductor with a large cross section given by $A_L = w_c m e$, where $m e$ represents the slot total height, will be compared to losses generated on a parallel of m conductors with cross section given by $A_m = w_c e$ (Figure 4).

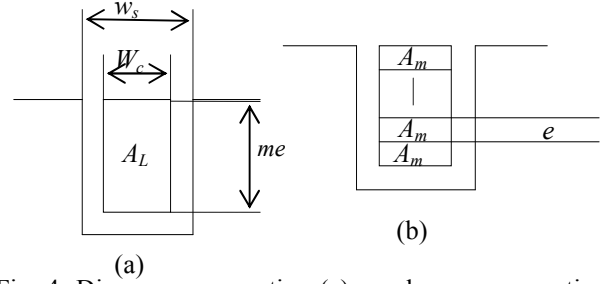


Fig. 4: Diagram representing (a) one large cross section conductor (b) m conductors of reduced cross section.

It is assumed that the m conductors are correctly transposed; hence the resistance of each one will be represented by (18). Moreover, under these conditions, the total current flowing in each m conductor will be I/m , being I the total current flowing in the large section conductor. Losses, P_L generated in the large section conductor, A_L , are given by:

$$P_L = \sum_{p=1}^m R_{DC_L} \varphi(\xi_L) I^2, \quad (20)$$

where: the subscript L refers variables to the dimensions of the large conductor.

Losses generated in the set on m transposed and paralleled conductors, P_m , will be given by the sum of losses generated in each conductor:

$$P_m = \sum_{p=1}^m R_{pT} \left(\frac{I}{m} \right)^2. \quad (21)$$

Attending that $R_{DCp} = m R_{DC_L}$ (21) is equivalent to:

$$P_m = R_{DC_L} \left(\varphi(\xi) + \frac{m^2-1}{3} \psi(\xi_m) \right) I^2, \quad (22)$$

where the subscript m refers the variable ξ to the dimensions of each m conductor.

Generically, losses can be represented by an addition of losses associated to the DC resistance of windings, $R_{DC} I^2$, and stray losses, P_s :

$$P = R_{DC} I^2 + P_s \quad (23)$$

Therefore, stray losses for the large conductor will be given by:

$$\frac{P_{PS_L}}{R_{DC_L} I^2} = \varphi(\xi_L) - 1 \quad (24)$$

and for the set of m parallel conductors by:

$$\frac{P_{S_m}}{R_{DC_L} I^2} = \varphi(\xi_m) + \frac{m^2-1}{3} \psi(\xi_m) - 1. \quad (25)$$

3.2.2 Results and Analysis

A graphical representation of the improvement in stray loss reduction, achieved by conductor's subdivision, is presented on Figure 5. Stray losses obtained under three possible conductor

subdivisions ($m=2, 3$ and 4) are represented in p.u. values of stray losses obtained under the reference situation, defined by one conductor ($m=1$) with $e=10$ mm, P_{Sm}/P_{SL} . Copper windings are assumed. Figure 5 shows that the reduction in stray losses achieved by large cross section conductors occurs only up to a certain frequency; for higher frequencies, conductor's subdivision becomes unfavourable, and this is due to the proximity effect of adjacent conductors. To exemplify this fact, stray loss generated on a set of m conductors, placed far enough from each other, meaning isolated from the magnetic field induced from adjacent conductor currents, were determined. Denoting these stray losses by $P_{Sm,isol}$, one obtains:

$$\frac{P_{Sm,isol}}{R_{DC} I^2} = \varphi(\xi_m) - 1. \quad (26)$$

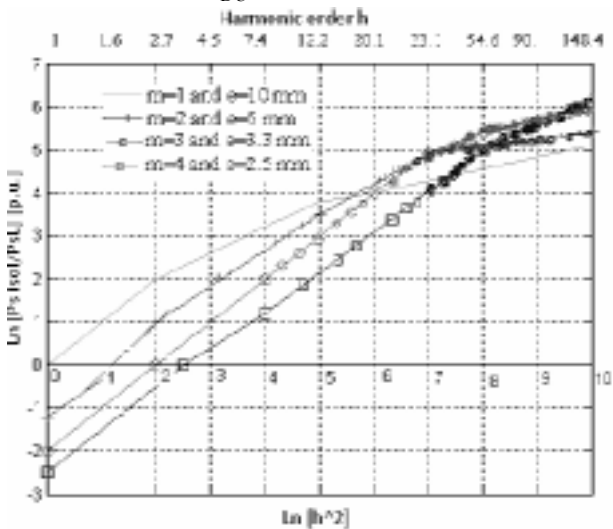


Fig. 5: Eddy losses variation with the number and width of conductors. The p.u. base is the eddy loss at rated frequency for one conductor with $e=10$ mm.

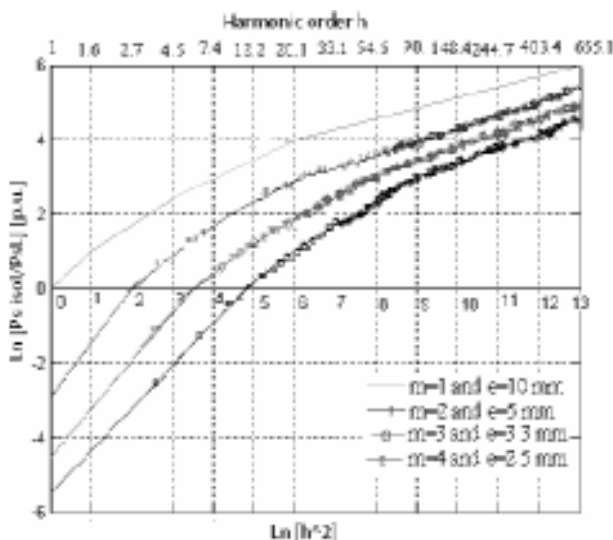
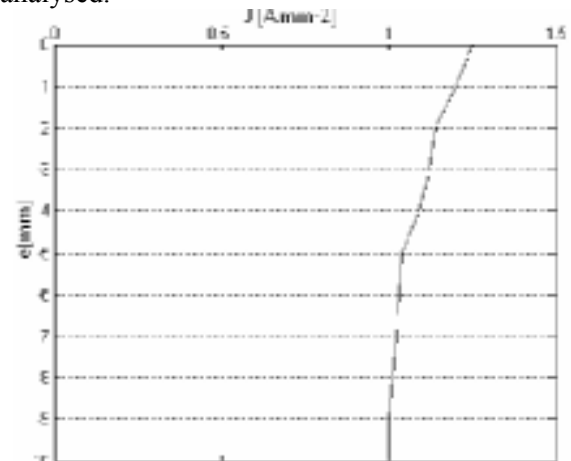


Fig. 6: Eddy loss variation with number and width of conductors, without considering proximity effect. The p.u. base is eddy loss at rated frequency for a conductor with $e=10$ mm.

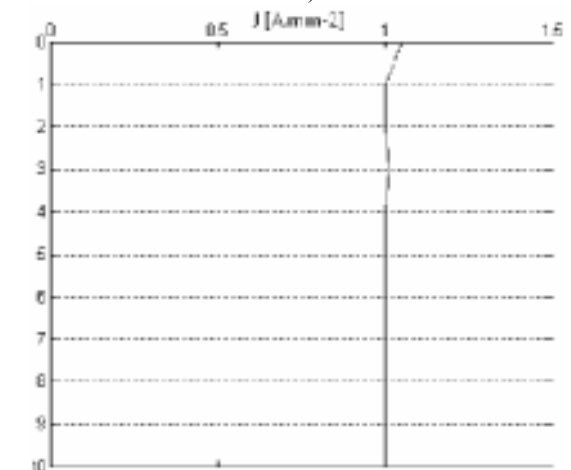
Graphical representation of (26) is presented on Figure 6.

Losses generated on the large section conductor ($m=1$ and $e=10$ mm) are exactly the same both on Figure 5 and Figure 6. On the other hand, losses generated on the set of m conductors are substantially reduced when the influence of adjacent conductors is not taken into consideration, Figure 6. These results can be confirmed from the study of current density distribution inside conductors, for the different analysed situations.

Figure 7 represents the amplitude of first harmonic ($h=1, f=50$ Hz) current density inside conductor cross section, for a total driven current of $I=100$ A. Three situations are considered: (a) a single large section conductor, (b) three equivalent conductors and (c) three equivalent conductors magnetically isolated from each other. The asymmetry that current density presents (skin effect) on the large section conductor, Figure 7 (a), is considerably reduced when the conductor is sub-divided, Figure 7 (b), and practically null if no proximity effects are considered, Figure 7 (c). A different situation occurs, when the effect of higher frequencies is analysed.



a)



b)

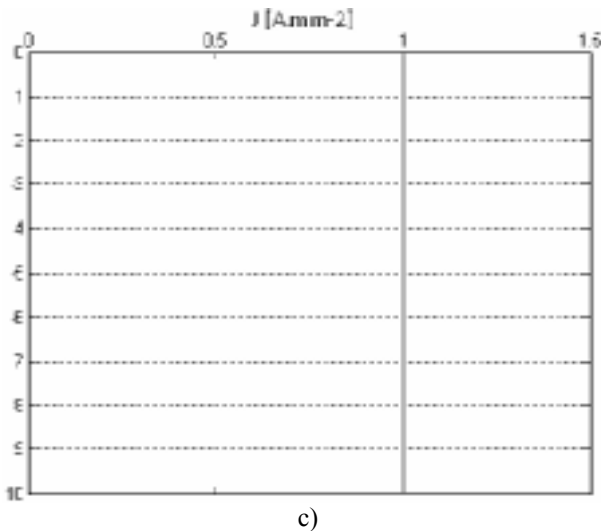


Fig. 7: Current density amplitude for $h=1$ and $I=100A$ (a) on one conductor with $e=10$ mm, (b) on 3 sub-conductors, considering proximity effect, (c) on 3 sub-conductors, without considering proximity effect.

Figure 8 represents current density amplitude for the conductors described above, but represents harmonic order $h=50$ ($f=2.5$ kHz): this value corresponds to a practical limit for significant detectable values in current harmonic spectrum.

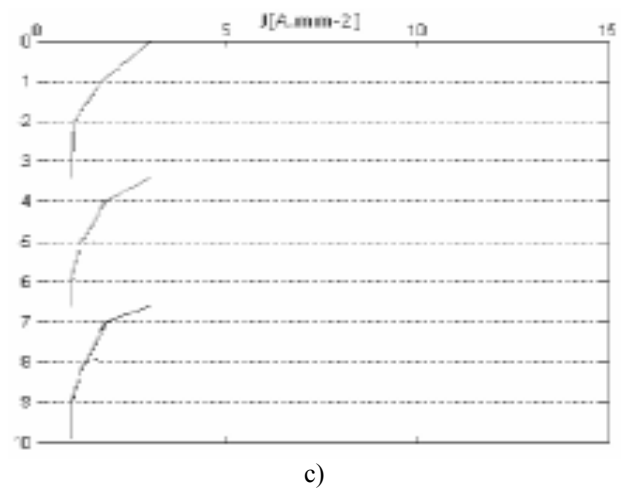
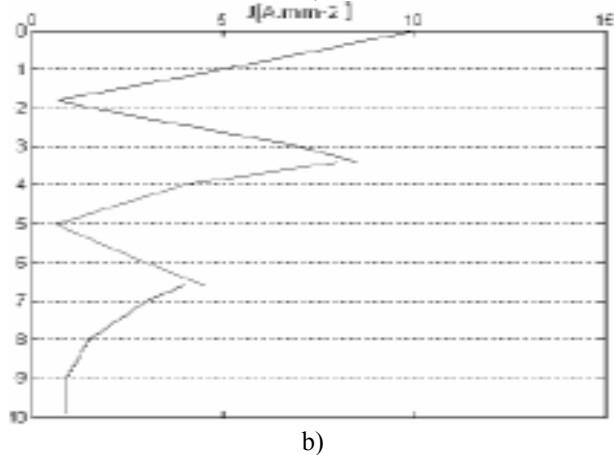
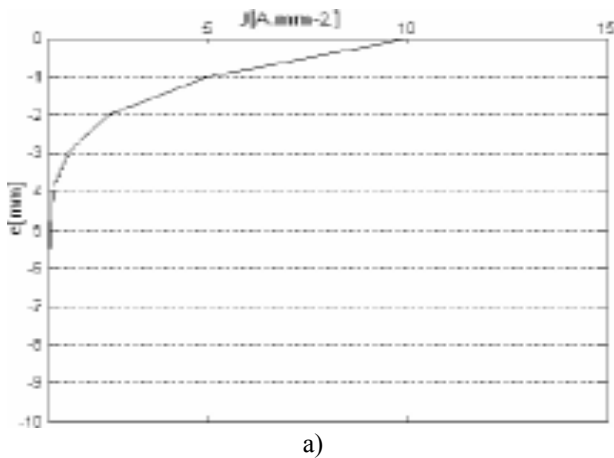


Fig. 8: Current density amplitude for $h=50$ and $I=100A$ (a) on one conductor with $e=10$ mm, (b) on 3 conductors, considering proximity effect, (c) on 3 conductors, without considering proximity effect.

Skin effect is more pronounced on the large section conductor, Figure 8 (a), but its sub-division does not lead to a more uniform distribution of current density. From the analysis of current density phase, one realises that, considering the influence of adjacent conductors, the current in the lower part of the uppermost conductors is antiphase with that in the higher part; proximity effect give rise to reverse currents inside upper conductors, Figure 8 (b). This asymmetry in current density leads to higher losses relatively to those generated on the single conductor, as represented on Figure 6. On the other hand, if conductors are assumed magnetically isolated, although skin effect occurs inside each conductor, the current density distribution is, in average and attending to graph scales, more uniform than in the large conductor, Figure 8 (c). The performed analysis leads to the conclusion that, sub-division of large cross section conductors, with correct transposition of sub-conductors, does reduce stray losses but only up to a certain frequency. For frequencies above, losses generated on the set of sub-conductors are higher than on a single conductor with an equivalent cross section, due to the proximity of adjacent currents.

3.3 Skin Effect in Transformer Windings

Expression (21) is commonly used for the evaluation of eddy-current loss in transformers driving sinusoidal currents and with rectangular cross section conductors [1],[10],[11].

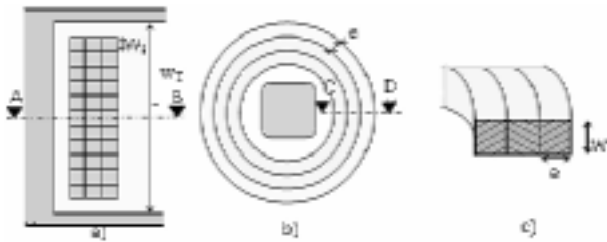


Fig. 9: (a) longitudinal section of transformer winding (one side) showing 3 layers and 11 turns per layer (b) view AB; cross section of transformer winding turn with 3 layers (conductors) (c) view CD; winding turn cross-section with 3 layers (conductors)

Considering a geometrical similitude between the slot and the transformer window, slot width, w_s , is replaced by the transformer window height, w_T , and conductors width, w_c , is replaced by the winding total height, Nw_i , where N represents the number of winding turns per layer and w_i a dimension of conductor cross section, according to Figure 9. Transformer winding diagram is represented on Figure 9. The winding equivalent resistance traducing alternating current effects (skin and proximity), R_{Ach} relatively to winding DC resistance, R_{DC} , will, then, be given by:

$$\frac{R_{Ach}}{R_{DC}} = \varphi(\xi) + \frac{m^2 - 1}{3} \psi(\xi) \quad (27)$$

where the reduced conductor width is:

$$\xi = \frac{e}{\delta} \sqrt{\frac{Nw_i}{w_T}} \quad (28)$$

and δ , the penetration deep, is given by (12). Practical application of (27) does require precise knowledge of winding geometry and construction procedures, data usually known by transformer manufacturer only and, not presented on the transformer data sheet. Moreover, calculations must be performed for each transformer winding. Obtained values must be reduced to a single side (HV or LV) of the transformer and then the total losses of all windings computed.

3.4 Asymptotic Tendencies

Although complex, the asymptotic behaviour of (27) can be studied from series expansion of hyperbolic trigonometric functions. For a clearer result, from (28) and (12) one can obtain [12],[13]:

$$\xi = e \sqrt{\frac{Nw_i}{w_T}} \sqrt{\frac{\gamma_w \mu_0 \omega_1}{2}} \sqrt{h} = \xi_1 \sqrt{h} \quad (29)$$

where ξ_1 represents the reduced conductor width, at fundamental frequency (section §3.1). The asymptotic study of (27) leads to:

$$\lim_{\omega \rightarrow 0} \left[1 + \frac{R_{Ach}}{R_{DC}} \right] = 1 + \frac{5m^2 - 1}{45} \xi^4 = 1 + \frac{5m^2 - 1}{45} \xi_1^4 h^2 \quad (30)$$

and

$$\lim_{\omega \rightarrow \infty} \left[1 + \frac{R_{Ach}}{R_{DC}} \right] = \left(1 + \frac{m^2 - 1}{3} \right) \xi = \left(1 + 2 \frac{m^2 - 1}{3} \right) \xi_1 \sqrt{h} \quad (31)$$

The asymptotic analysis allows the conclusion that the increase in the transformer equivalent resistance follows a quadratic behaviour for reduced harmonic orders but after a so-called transition frequency, this behaviour becomes a square root. Limits traduced by (30) and (31) are represented on Figure 10 for six different values of the conductor width, and for a constant number of parallel conductors ($m=20$). On this diagram, a straight line with 45° slope traduces a quadratic increase of eddy losses with frequency (or harmonic order). It is interesting to remark that the transition frequency (the frequency at which the quadratic effect verified for lower orders ceases) is reduced as the conductors width is increased.

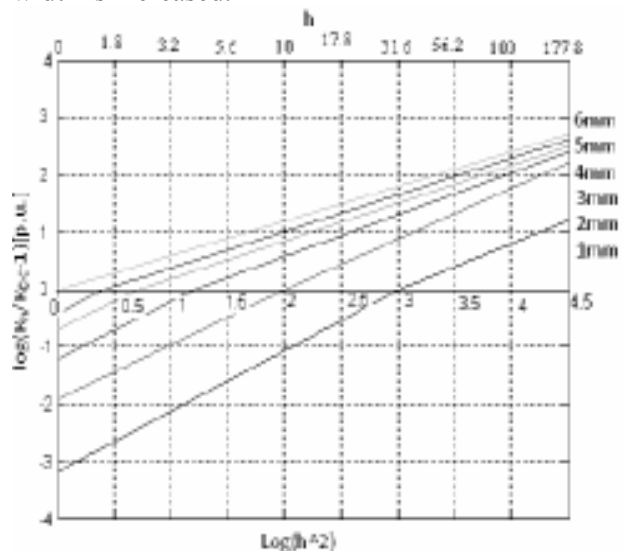


Fig. 10: Eddy loss increase with frequency for different conductor's width and in p.u. values of eddy losses at rated frequency on the set of m conductors with 6 mm width.

4 Stray Loss Models

Network managers do have to deal with harmonic effects in distribution transformers; model (27) is, however, of reduced usefulness for this application due to the number of its parameter. To study losses due to non-sinusoidal load currents in a generic way, it would be useful to derive a general formulation, quite simple, but easily parameterised and valid for a given range of rated power transformers.

4.1 Existing Models

One can find in specialised literature some empirical formulae to approximate expression (27), [14],[15]. Most of the proposed formulae are valid only within a limited range of frequencies. In fact they overweight losses due to higher, frequencies since they assume only the quadratic increase of stray losses with frequency. These simplified formulas are derived by approximating functions $\varphi(\xi)$ and $\psi(\xi)$, (14) to a limited number of terms of their series development.

$$\varphi(\xi) \approx 1 + \frac{4}{45}\xi^4 \quad \text{and} \quad \psi(\xi) \approx \frac{1}{3}\xi^4 \quad (32)$$

By inserting (32) into (27) one obtains:

$$\frac{R_{Ach}}{R_{DC}} = 1 + \frac{5m^2 - 1}{45}\xi^4 \quad (33)$$

which, attending to (29), can be rewritten as:

$$\frac{R_{Ach}}{R_{DC}} = 1 + \frac{5m^2 - 1}{45}\xi_1^4 h^2 \quad (34)$$

The validity of approximations (32) is strictly dependent upon the conductor reduced width, ξ , which in turn, is a function of geometric dimensions and frequency. To realise the magnitude of the performed approximation, two numerical examples are presented, Figure 11. Figure 11 (a) and (b) represents expression (27), denoted as "Original", and its "Approximation" given by (34), for copper conductors with width 10 mm and 3 mm, respectively. Figure 11 is illustrative of the frequency domain reduction for the validity of approximation (34), as the conductor width increases.

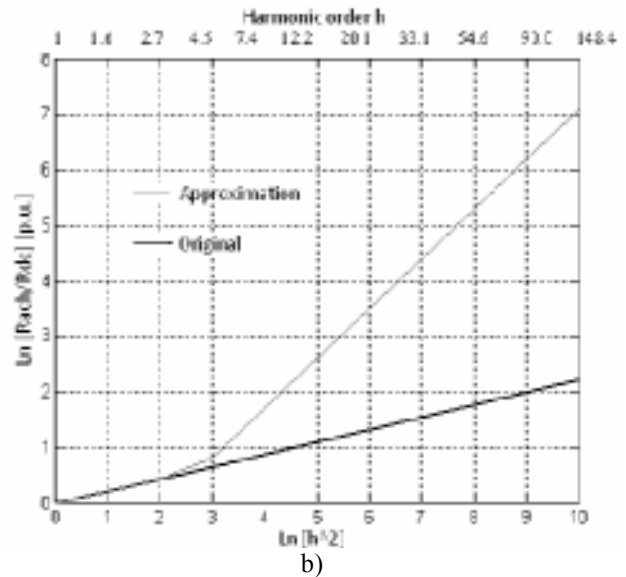
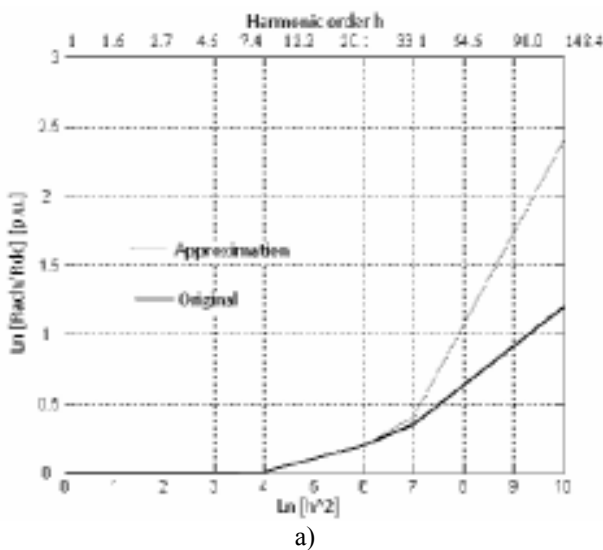


Fig. 11: Eddy loss evaluated with expression (27) and (34) for one conductor with with (a) 10 mm and (b) 3 mm.

Simplified models based on approximation from Taylor series development, are the most common ones, [1],[4],[9], and can be rewritten as:

$$R_{Ach} = R_{DC} \left(1 + \frac{\Delta R_h}{R_{DC}} \right) \approx R_{DC} (1 + s_{1DC} h^2) \quad (35)$$

where s_{1DC} represents the ratio of windings stray losses at rated frequency to losses associated to the DC resistance or, in other words, the additional losses associated to the DC resistance, due to effects of sinusoidal current at rated frequency.

$$s_{1DC} \equiv \frac{\Delta R_h}{R_{DC}} \Big|_{h=1} \quad (36)$$

Models of the form,

$$R_{Ach}(h) \approx R_{DC} (1 + s_{1DC} \sqrt{h}) \quad (37)$$

will underestimate lower harmonic orders.

Other proposed models, [6], [7], take into consideration that windings and non-windings stray losses increase differently with harmonic order and are, generically, of the form:

$$R_{Ach}(h) \approx R_{DC} (1 + s_{1DC} h^q + (1 - s_{1DC}) h^r) \quad (38)$$

where exponents q and r are obtained by fitting data values from particular situations. Such a model does not, as well, fulfil the asymptotic higher and lower order tendencies. Moreover, q and r -values are dependent from each analysed situation (harmonic spectrum contents), since a high harmonic spectrum will lead to q values closer to 2 and with a lower one, the obtained q values will tend to $1/2$ (asymptotic tendency [7]).

4.2 Proposed Model

According to [5],[16],[17],[18] stray losses on windings are the most important due to the corresponding increase in transformer temperature. Therefore, these are the only harmonic stray losses this work will consider. To model the effects of non-sinusoidal currents on MV/LV (medium voltage/low voltage) distribution transformers, this work proposes the following model [6], which verifies the skin effect asymptotic tendency:

$$\frac{R_{ACh}}{R_{DC}} \equiv \beta_h = \frac{1 + g + g^3}{1 + g^2} \quad (39)$$

with,

$$g^2 \approx \zeta(S_R)h \quad (40)$$

where $\zeta(S_R)$ represents a generic function of transformer rated power, S_R [VA]. From (39) and (40), one can verify that the asymptotic tendency is fulfilled since:

$$\lim_{h \rightarrow 0} \beta_h = 1 \quad (41)$$

and

$$\lim_{h \rightarrow \infty} \beta_h = \sqrt{\zeta(S_R)}\sqrt{h} \quad (42)$$

To determine function $\zeta(S_R)$, expressions (31) and (42) must be compared to conclude that it must be:

$$\sqrt{\zeta(S_R)} \propto \left(1 + 2\frac{m^2 - 1}{3}\right) \xi_1 \quad (43)$$

Attending that ξ_1 is function of the conductors width, e , (29), two extreme scenarios must be analysed. A homogeneous transformer series (similar manufacturer structure and different rated powers) will be considered. Current density, used in the series, will be assumed constant, which is a common occurrence in practice, since it corresponds to the maximisation of materials performance. The ratio $\sqrt{Nw_i/w_T}$ will be considered as constant, also.

i) On the first scenario the conductors width will be considered constant and thus, the constant current density with increasing transformer rated power, imply a corresponding increase in the number of parallel conductors m .

ii) On the second scenario, the opposite situation occurs: the number of parallel conductors will be kept constant and the conductor's height will increase with the transformer rated power, in such a way, that the transformer rated current density can also be kept constant.

For the first scenario, if one assumes that the number of parallel conductors will increase proportionally to the transformer rated power, meaning $m \propto S_R$, expression (43) leads to:

$$\sqrt{\zeta(S_R)} \propto 2\frac{S_R^2 - 1}{3} \Leftrightarrow \zeta(S_R) \propto S_R \quad (44)$$

For the second scenario, if one assumes that, to the necessary increase in the conductors height corresponds a proportional increase in short-circuit losses, meaning $e \propto P_{cc}$, similitude relationships, lead to $e \propto S_R^{3/4}$ at constant rated density current. Therefore, the (43) proportionality relationship will be equivalent to:

$$\sqrt{\zeta(S_R)} \propto \xi_1 \propto e \Leftrightarrow \zeta(S_R) \propto S_R^{3/2} \quad (45)$$

Neither of these two extreme situations is expected to represent the reality, since a combination of both often occurs in practice. For a given number of parallel conductors, their width is expected to increase up to a certain rated power. Above that power, conductors are subdivided (increase in m) and then again, increase in power will be achieved by an increase of the conductor's height. A possible generic function accomplishing (44) and (45) can be defined as:

$$\zeta(S_R) \equiv \Gamma \left(\frac{S_R}{S_{R_0}}\right)^k \quad \text{with } 1 < k < \frac{3}{2} \quad (46)$$

Therefore, the proposed model assumes the following form:

$$g^2 \approx \zeta(S_R)h \equiv \Gamma \left(\frac{S_R}{S_{R_0}}\right)^k h \quad \text{with } 1 < k < \frac{3}{2} \quad (47)$$

where: S_{R_0} reference transformer rated power [kVA], Γ empirical proportionality coefficient [dimensionless].

The proposed model takes the form of a general similitude relationship and the Γ empirical coefficient value will validate the relationship for a given range of transformers rated power. Main advantages introduced by the proposed model are: to fulfil the asymptotic tendency both for lower and higher harmonic orders, avoiding the unrealistic explosion of higher harmonic losses [7] verified on models where the losses are proportional to h^2 (35), and avoiding the underestimation of lower harmonic losses as do models with losses proportional to \sqrt{h} (37). Moreover, model parameterisation becomes easy, since it relies on the transformer rated power only, traducing transformers different sensitivities to stray losses with its rated power. The present work is focused, mainly, on distribution transformers. Therefore, and on the lack of other experimental data, values referred on [5] were used to "tune" the proposed model. Model proposed by [5] is:

$$\frac{R_{Ach}}{R_{Ach}|_{h=1}} \approx 1 + s_{1AC}(h-1)^d \quad (48)$$

where $R_{Ach}|_{h=1}$ represents winding resistance (DC and AC effects) at rated frequency, d is an exponent with a value about 1.6 for distribution transformers, according to an European manufacturer and s_{1AC} (losses at harmonic h referred to losses at fundamental frequency) is a coefficient, with typical values given in the same reference, for power distribution transformers rated from 200 kVA to 2000 kVA. Model (48) can not be directly compared to (39) model. However, considering that the loss component due to stray effect is around 10% of total load loss at rated frequency, it can be derived:

$$R_{DC} \approx \frac{9}{10} R_{Ach}|_{h=1} \quad (49)$$

and thus expression (48) takes the desired form of:

$$R_{Ach} \approx \frac{10}{9} R_{DC} [1 + s_{1AC}(h-1)^d] \quad (50)$$

Model tuning will be performed for the lower harmonic orders since, according to the asymptotic study; the model proposed [5] overestimates higher orders. The reference transformer rated power, S_{R0} , is 1 000 kVA, to be almost in the middle point of the considered power range, 200 kVA to 2 000 kVA. The minimisation of errors between the proposed and Lehtonen models, for the fifth harmonic, attending to the k restriction in (47) and considering also $\Gamma > 0$, leads to the values of Γ and k parameters listed in Table 1:

Table 1: Values of Γ and k parameters.

Trans, rated power [kVA]	200	500	800	1000	1600	2 000
Γ	0.66	0.61	0.77	0.74	0.68	0.66
k	3/2	3/2	3/2	3/2	3/2	3/2

The proposed model will, then, be defined by (39) and (40), with:

$$g^2 \approx \frac{2}{3} \left(\frac{S_R}{S_{R0}} \right)^{3/2} h \quad (51)$$

Figure 12 represents comparisons between the proposed and the reference [5] models, where differences are clearly seen. By comparing Figure 11 and Figure 12, similitude behaviour between lines representing "Original" expression, (27), and "Proposed model", (51), as well as between "Approximated" expression, (34), and "[5] model" (50), can be found. The next section will present some simulation results of transformer loss of life, using the proposed model to represent the transformer losses under non-sinusoidal.

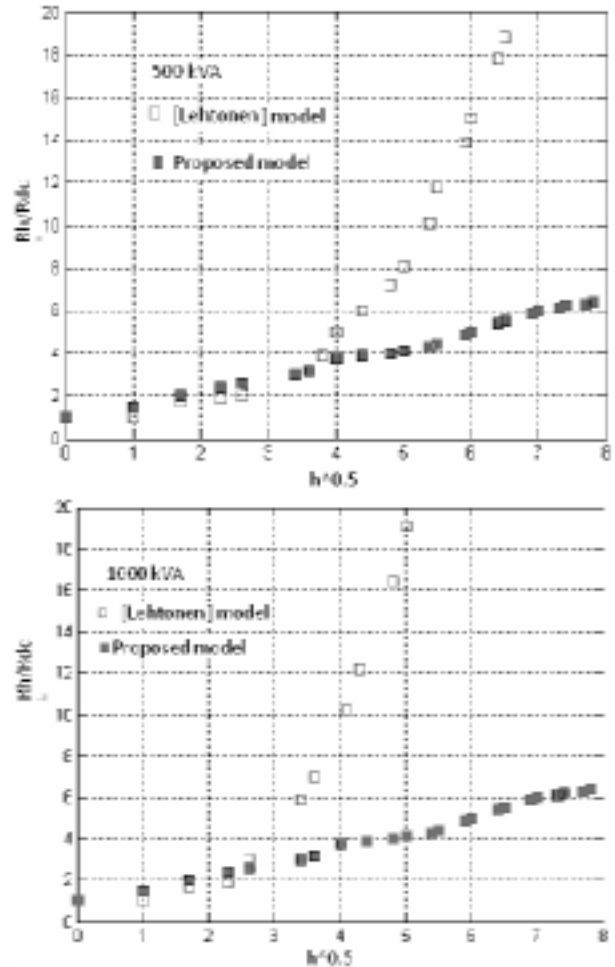


Fig. 12: Comparison between proposed and Lehtonen [5] model, for a 500 kVA and a 1000 kVA transformer.

3 Conclusions

To estimate correctly transformer loss of life (or, reciprocally, its power derating), it is necessary to take into account the harmonic currents spectrum, the electrical characteristics (losses), the thermal behaviour (thermal model) and the realistic load and ambient temperature profiles (variability). Transformer loss of life decreases when driving distorting loads, since additional losses are generated that lead to an increase in the transformer hot-spot temperature. Due to the losses increase with frequency, additional losses must be taken into consideration on loss of life estimations, mainly if transformer is driving highly distorting loads. Correct estimation of additional losses is complex since it requires a precise knowledge of transformer manufacturing procedures and parameters, such as: winding structure, conductor dimensions and magnetic circuit geometry. Complex models are useful if transformer magnetic and electrical circuits are fully specified both on its physical and

geometrical characteristics. Correct estimation of transformer additional losses requires heavy parameterisation and medium complexity calculation tools. Simplified models of easy parameterisation are commonly used. However, they do not fulfil the asymptotic behaviour introduced by considering the skin and proximity effects. Some models underestimate low order harmonics, others overweight high order harmonics. A new model was proposed and parameterised only with transformer rated power. This new model fulfils asymptotic tendencies both for low and high order harmonics and takes into consideration the current harmonic spectrum and the transformer rated power sensitivity to distorting loads. From simulations, it has been shown that, for realistic distorting loads, transformer thermal loss of life can approximately be determined from the total harmonic distortion factor of the current, once the load linear component and the ambient temperature profiles has been characterised. For deterministic time varying profiles, characteristics of realistic input profiles, such as amplitude, frequency variability and the correlation degree between them, are aspects that can not be neglected and, in practice, may have a greater influence than additional distorting loads, for a correct estimation of transformer expected life.

References

- [1] Crepaz S., *Electrical Insulation Deterioration Treated as a Chemical Rate Phenomenon*, AIEE Transaction, Vol. 67, pp.113-122, 1948.
- [2] Degeratu Pr., Popescu M.C., Boteanu N., *The optimization of the acting which must achieve a speed variation, taking into account the criterion of energy losses. The quality of the obtained results.* International Conference on Applied and Theoretical Electricity, pp. 427-431, Craiova, 2000.
- [3] IEC-76, Part 2, International Electrotechnical Commission, *Power Transformers Temperature Rise*, Second Edition, 1993.
- [4] IEC-354, International Electrotechnical Commission, *Loading Guide for Oil-Immersed Power Transformers*, Second Edition, 1991.
- [5] Lehtonen M., *Harmonic losses and the local carrying capacity of power systems components in industrial networks*, Report CIRED'91, Liege, pp.1-6, 1991.
- [6] Resende M.J., Pierrat L., Santana J., *Sensitivity Analysis as Accuracy Measure of Simplified Strongly Non-Linear Thermal Model Transformers Reliability Studies*, 2nd International Symposium on Sensitivity Analysis of Model Output, pp.227-230, Venice, 1998.
- [7] Pierrat L., *Méthode d'Identification et Analyse d'Incertitude pour les Paramètres d'une Courbe d'Echauffement Tronquée*, 8th International Congress of Metrology, Besacon, 1997.
- [8] Bulucea C.A., Nicola D.A., *Introduction in Electrotechnics and Electrical equipments*, SITECH Publishing House, pp.25-38, 2004.
- [9] Karsai K., Kerényi D., Kiss L., *Large Power Transformers*, Elsevier Science Publishers, Amsterdam, The Netherlands, 1987.
- [10] Mastorakis N.E., Bulucea C.A., Manolea G., Popescu M.C., Perescu-Popescu L., *Model for Predictive Control of Temperature in Oil-filled Transformers*, Proceedings of the 11th WSEAS International Conference on Automatic Control, Modelling and Simulation, ISSN: 1790-5117, ISBN: 978-960-474-082-86, pp.157-165, Istanbul, Turkey, May 30-June1, 2009.
- [11] Popescu M.C., Mastorakis N.E., Bulucea C.A., Manolea G., Perescu-Popescu L., *Transformer Model Extension for Variation of Additional Losses with Frequency*, Proceedings of the 11th WSEAS International Conference on Automatic Control, Modelling and Simulation, ISSN: 1790-5117, ISBN: 978-960-474-082-86, pp.166-171, Istanbul, Turkey, May 30-June1, 2009.
- [12] Mastorakis N.E., *On the Solution of Ill-Conditioned Systems of Linear and Non-Linear Equations via Genetic Algorithms (GAs) and Nelder-Mead Simplex Search*, WSEAS Transactions on Information Science and Applications, Issue 5, Volume 2, 2005, pp. 460-466.
- [13] Mastorakis N.E., *Numerical Solution of Non-Linear Ordinary Differential Equations via Collocation Method (Finite Elements) and Genetic Algorithm*, WSEAS Transactions on Information Science and Applications, Issue 5, Volume 2, 2005, pp. 467-473.
- [14] Popescu M.C., *Simularea numerică a proceselor*, Reprografia Universității C. Brancuși, Targu Jiu, pp.45-67, 1996.
- [15] Popescu M.C., Olaru O., Mastorakis N.E., *Equilibrium Dynamic Systems Intelligence*, WSEAS Transactions on Information Science and Applications, ISSN: 1790-0832, Issue 5, Volume 6, pp.725-735, May 2009.
- [16] Popescu M.C., Balas V., Manolea G., Mastorakis N.E., *Regional Null Controllability for Degenerate Heat Equations*, Proceedings of the 11th WSEAS International Conference on Sustainability in Science Engineering, ISSN: 1790-2769, ISBN: 978-960-474-080-2, pp.32-37, Timisoara, Romania, May 27-29, 2009.
- [17] Popescu M.C., *Simularea frecvenței de excitație periculoasă în cazul fenomenului de rezonanță*, Sesiunea Științifică „Echipamente electromecanice”, Facultatea de Electromecanică, Craiova, 1994.
- [18] Nicola D.A., Bulucea C.A. *Electrotechnics, Electrical Equipments and Machines*, SITECH Publishing House, pp. 235-252, 2005.